



Greenland climate simulations show high Eemian surface melt

Andreas Plach^{1,2,3}, Bo M. Vinther⁴, Kerim H. Nisancioglu^{1,5}, Sindhu Vudayagiri⁴, and Thomas Blunier⁴

¹Department of Earth Science, University of Bergen and Bjerknes Centre for Climate Research, Bergen, Norway

²Department of Meteorology and Geophysics, University of Vienna, Austria

³Climate and Environmental Physics, Physics Institute, University of Bern, Switzerland

⁴Centre for Ice and Climate, Niels Bohr Institute, University of Copenhagen, Denmark

⁵Centre for Earth Evolution and Dynamics, University of Oslo, Oslo, Norway

Correspondence: Andreas Plach (andreas.plach@gmail.com)

Abstract. This study presents simulations of Greenland surface melt for the Eemian interglacial period (~130000 to 115000 years ago) derived from regional climate simulations with a coupled surface energy balance model. Surface melt is of high relevance for ice core records because it can influence observations, e.g., lower the preserved total air content (TAC) used to infer past surface elevation. An investigation of surface melt is particularly interesting for warm periods, such as the Eemian interglacial period, with enhanced surface melt. Furthermore, Eemian ice is the deepest and most compressed ice preserved on Greenland, which means that melt layers can not be identified visually. Therefore, a knowledge of potential melt layers would be advantageous. The simulations presented here show Eemian surface melt at all deep Greenland ice core locations. Estimated TAC, based on simulated melt during the Eemian, could explain the lower TAC observations: at the summit of Greenland (GRIP) a refreezing ratio of more than 25 % of the annual accumulation is simulated. As a consequence, elevated levels of surface melt during warm periods should be considered when interpreting Greenland TAC measurements as surface elevation changes. Additionally to estimating the influence of melt on past TAC in ice cores, the simulated surface melt could also be used to identify potential coring locations where Greenland ice might be best preserved.

1 Introduction

The Eemian interglacial period (~130000 to 115000 years ago; thereafter ~130 to 115 ka) was the last period with a warmer-than-present summer climate on Greenland (CAPE Last Interglacial Project Members, 2006; Otto-Bliesner et al., 2013; Capron et al., 2014). Favourable orbital parameters (higher obliquity and eccentricity compared to today) during the early Eemian period caused a positive Northern summer insolation anomaly (and negative winter anomaly) at high latitudes, which led to a stronger seasonality (Yin and Berger, 2010). A stronger seasonality with relatively warm summer seasons is favourable for surface melt of the Greenland ice sheet.

Unfortunately, the presence of surface melt during ice formation can be a problem for the integrity of ice core records. Measurements of CH₄, N₂O, and total air content (TAC) can be influenced if the ice core contains melt layers. Other ice core measurements such as $\delta^{18}\text{O}$, δD , and deuterium excess appear to be only marginally affected (NEEM community members, 2013). However, melt layers have the potential to form impermeable layers and also influence the diffusion of ice core signals.



The observed TAC of ice core records is the only direct proxy for past surface elevation, i.e., the TAC is governed by the density of air which mainly decreases with elevation. However, TAC was also found to have an insolation signal in East Antarctica (Raynaud et al., 2007) and Greenland (Eicher et al., 2016). While TAC can be applied on each individual ice core without the need for other reference ice cores, another indirect method which has been applied to infer Holocene thinning of the Greenland ice sheet (Vinther et al., 2009) requires several ice cores. Vinther et al. (2009) compare the changes of $\delta^{18}\text{O}$ at coastal ice caps (stable surface elevation due to confined topography) with Greenland deep ice cores, and infer elevation changes. Unfortunately, Eemian ice core records are sparse, and therefore TAC is the only method available to estimate surface elevation changes this far back in time. Since the assumed surface elevation also influences the actual Eemian temperature reconstructions and its uncertainty range, an accurate TAC record is of high importance. The following example illustrates this importance: the NEEM-derived surface temperature anomaly (NEEM community members, 2013) at 126 ka is $7.5 \pm 1.8^\circ\text{C}$ without accounting for elevation changes; including the elevation change based on TAC measurements, the temperature estimate becomes $8 \pm 4^\circ\text{C}$. This means that more than half of the uncertainty of this temperature estimate is related to the uncertainty of past surface elevation. Despite these concerns, the number of studies investigating the frequency of melt layers in Greenland ice cores is small (Alley and Koci, 1988; Alley and Anandakrishnan, 1995).

This study investigates regional climate simulations and observations at six deep Greenland ice core sites — Camp Century, Dye-3, EGRIP, NEEM, NGRIP, GRIP (used synonymous with GISP2 due to their close proximity). Furthermore, an ice cap in the vicinity of the Greenland ice sheet is investigated — the Agassiz ice cap. TAC is derived from the regional climate simulations at these seven locations of interest also considering the simulated melt (Sec. 2). Furthermore, the simulated temperature and melt at the locations is validated, and the impact on TAC is estimated and compared with ice core observations (Sec. 3 and 4). The results indicate that Greenland ice core records from warm periods, such as the Eemian interglacial period, might be more influenced by surface melt than previously considered (Sec. 5).

2 Methodology

Climate and surface mass balance (SMB) simulations

This study uses climate and surface mass balance (SMB) based on Eemian time slice simulations with a fast version of the Norwegian Earth System Model (NorESM1-F; Guo et al., 2018) representing 125 and 115 ka conditions (and a pre-industrial control simulation). These global simulations are dynamically downscaled over Greenland with the regional climate model Modèle Atmosphérique Régional (MAR), which was extensively validated over Greenland (Fettweis, 2007; Fettweis et al., 2013, 2017). All climate simulations use an offline, modern ice sheet, in lack of a reliable Eemian ice sheet estimate. However, the orbital forcing and the greenhouse gas concentrations are changed in the four Eemian experiments. The SMB used in this study is derived from a full surface energy balance (SEB) model coupled to MAR.

This SEB-derived SMB is also analyzed in a study investigating the influence of climate model resolution and SMB model selection on the simulation of the Eemian SMB (Plach et al., 2018a) which amongst other things shows the high importance of considering solar insolation in Eemian simulations. Additionally, the SEB-derived SMB shows less extensive Eemian melt

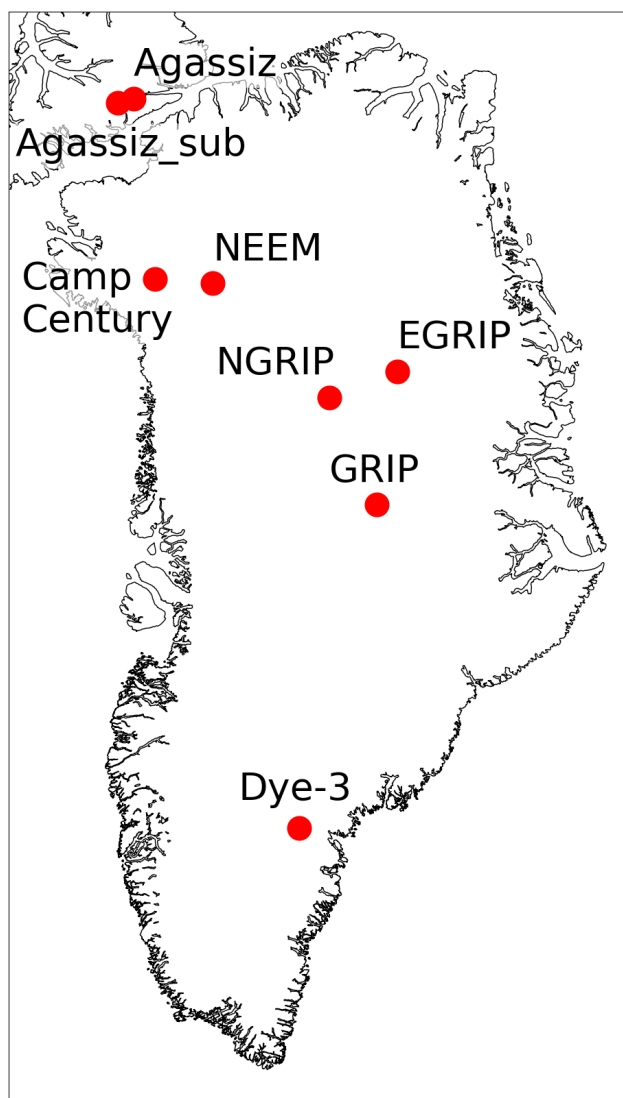


Figure 1. Overview map of Greenland ice core locations discussed in this study. Note: Agassiz_sub refers to a substitute location of the Agassiz ice cap used due to the model topography misrepresentation (see Sec. 2).

than an intermediate complexity SMB model while using the most complete representation of physical surface processes in the investigated model pool.

Furthermore, the discussed SMB is also used in a study investigating the Eemian Greenland ice sheet with an higher-order ice sheet model (Plach et al., 2019). Plach et al. (2019) shows that different external SMB forcings show a bigger influence on the Eemian ice volume minimum than sensitivity tests with internal ice dynamical parameters like basal friction. The ice sheet simulations with the SEB-derived SMB showed a moderate smaller Eemian ice sheet equivalent to ~0.5 m of sea level rise.



Table 1. Greenland ice core locations.

location	latitude (°N)	longitude (°W)	observed elevation (m)	model elevation (m)
Agassiz	80.81	72.89	1760	1354
Agassiz_sub	80.53	74.45	1760	1741
Camp Century	77.16	61.13	1885	1776
Dye-3	65.18	43.81	2489	2444
EGRIP	75.63	35.99	2708	2684
NGRIP	75.10	42.32	2917	2906
NEEM	77.45	55.06	2450	2253
GRIP	72.58	38.63	3230	3198

Agassiz_sub refers to a substitute location used due to the model topography misrepresentation.
 See Sec. 2 for further explanation.

In this study, the SEB-derived SMB simulations are analyzed at six deep Greenland ice core locations — Camp Century, Dye-3, EGRIP, NEEM, NGRIP, GRIP — and an adjacent ice cap — the Agassiz ice cap (Fig. 1). Due to model topography misrepresentation at the ice sheet margins, i.e., the model topography is lower than in reality at the Agassiz ice cap location (model resolution 25 km), a substitute location (Agassiz_sub) in the vicinity of the ice cap, with a model elevation similar to the observed elevations, is chosen (Tab. 1).

Observed surface melt

The pre-industrial regional climate and SMB simulations are validated against satellite and temperature observations at the locations of interest. The two observational melt day data sets are both derived from satellite-borne passive microwave radiometers — Scanning Multichannel Microwave Radiometer (SMMR), the Special Sensor Microwave/Imager (SSM/I), and the Special Sensor Microwave Imager/Sounder (SSMIS). The first data set, *MEASUREs (Greenland Surface Melt Daily 25km EASE-Grid 2.0, Version 1)*, covers the years 1979 to 2012 and is available for the entire Northern Hemisphere. The melt onset is identified by comparing 37 GHz, horizontally polarized (37 GHz H-Pol) brightness temperatures with dynamic thresholds associated with a melting snowpack (Mote, 2014). Unfortunately, the Agassiz ice cap is not covered by this data set. The second data set, $T19H_{melt}$, covers May through September for most years between 1979 to 2010 on the 25 km MAR grid. It uses data collected at K-band horizontal polarization (T19H) with a constant brightness temperature threshold of 227.5 K (Fettweis et al., 2011). Both satellite data sets are discussed to show their different sensitivities and to illustrate the uncertainty of these satellite-based melt observations.

The seasonal temperature observations at weather stations and 10 m borehole temperatures (representing annual mean temperatures) are taken from a collection of shallow ice core records and weather station data (Faber, 2016). Finally, the bore hole temperatures from the Agassiz ice cap are taken from Vinther et al. (2008).



Observed total air content (TAC)

Firstly, the Dye-3 TAC for the ice core depth range of ~240 to 1920 m was extracted from Herron and Langway (1987, Fig. 4 therein). Since Souchez et al. (1998) indicate that ice from warmer periods (higher δO^{18} values), likely Eemian, is located below 2000 m at Dye-3, the presented Dye-3 TAC record does not represent Eemian conditions. Secondly, the NEEM TAC observations (NEEM community members, 2013) cover the deepest section of the NEEM ice core from ~2200 to 2500 m depth (corresponding to an age of ~75 to 128 ka; not continuous) and an example for Holocene conditions from depths between ~100 to 1400 m (no age provided). Thirdly, the NGRIP TAC record (Eicher et al., 2016) includes the entire core from ~130 to 3080 m, however the sampling resolution varies. An age model is provided for the entire data set with an oldest age of ~120 ka. Finally, the GRIP TAC data set (Raynaud, 1999) covers depths from ~120 to 2300 m and ~2780 to 2909 m, while an age model is only provided for the upper part (oldest ice 41 ka). For the deeper sections of the core, a published unfolding of the GRIP core (Landais et al., 2003, age bands in Fig. 3 therein) is used to assign an age to the observations. Note that only the Eemian sections for NEEM, GRIP, and NGRIP are shown in Fig. 7.

The Eemian ranges in Fig. 6 are calculated as the mean (plus/minus two standard deviations) of the lowest 10 % of observed Eemian TAC (Fig. 7; used observations are indicated in orange) for NEEM and NGRIP. Due to the low number of Eemian observations at GRIP, a different threshold of 20 % is used for this core. For the calculation of the late Holocene ranges in Fig. 6, observations younger than 1000, 2000, and 4000 years, are used for GRIP, Dye-3, and NGRIP, respectively. The late Holocene range for NEEM is calculated from the entire Holocene example provided in the NEEM community members (2013) data (nine data points; no age provided).

Calculation of the model-derived total air content (TAC)

The model-derived TAC is calculated with the annual mean surface pressure and the annual mean near-surface temperature from the MAR regional climate simulations at every location of interest (Martinerie et al., 1992; Raynaud et al., 1997):

$$TAC = V_c \frac{P_c T_0}{T_c P_0} \quad (1)$$

where V_c is the pore volume at close-off in cm^3/g of ice, P_c the mean atmospheric pressure at the elevation of the close-off depth interval in mbar , T_c the firn temperature prevailing at the same depth interval in K , P_0 the standard pressure (1013 mbar), and T_0 the standard temperature (273 K). V_c is calculated as a function of T_c following an empirical relation (Martinerie et al., 1994; Raynaud et al., 1997):

$$V_c = (6.95 \times 10^{-4} T_c) - 0.043 \quad (2)$$



110 This theoretical TAC is then reduced (TAC_{red}) depending on the percentage of refreezing of the annual accumulation (RZ_{per}):

$$TAC_{red} = TAC \times \left(1 - \frac{RZ_{per}}{100}\right) + TAC_{refrozen} \times \left(\frac{RZ_{per}}{100}\right) \quad (3)$$

where $TAC_{refrozen}$ is calculated using Henry's solubility law (Sander, 2015) for N_2 and O_2 (neglecting other atmospheric gases) to account for air that is dissolved in the meltwater before refreezing:

$$115 \quad TAC_{refrozen} = C_{a,N_2} + C_{a,O_2}, \quad (4)$$

with C_{a,N_2} , and C_{a,O_2} being the aqueous-phase concentration of N_2 and O_2 , respectively:

$$C_{a,N_2} = P_c * C_{atm,N_2} * H^{cp,N_2} \quad (5)$$

and

$$C_{a,O_2} = P_c * C_{atm,O_2} * H^{cp,O_2} \quad (6)$$

120 where C_{atm,N_2} and C_{atm,O_2} are the atmospheric concentration ratio (0.79 and 0.21) and H^{cp,N_2} , H^{cp,O_2} are Henry's solubility constants (10.49×10^{-6} and 2.1982×10^{-5}) for N_2 and O_2 , respectively.

3 Results

Temperatures

The simulated pre-industrial annual mean (near-surface) temperatures at the seven locations of interest (Fig. 2; black columns; 125 short bold lines - ensemble means; short thin lines - individual model years) generally fit well with annual mean temperature observations from weather stations (Fig. 2; long bold lines in black; standard deviation in gray shading). However, the annual means inferred from 10 m borehole temperatures (Fig. 2; long bold lines in gray) are consistently colder than the simulated pre-industrial means. The lower borehole temperatures are probably related to the fact that they represent surface temperatures which are typically lower than near-surface temperatures. Only at the Agassiz site, the borehole temperatures are higher than 130 the simulated temperatures. This exception is likely related to the usage of a substitute location (see Sec. 2).

The annual mean temperatures at most locations only vary by 0.5 °C between the time slice simulations, i.e., a strong difference between the pre-industrial (Fig. 2; black) and warm Eemian simulations (Fig. 2; red and orange) is absent in the climate simulations.

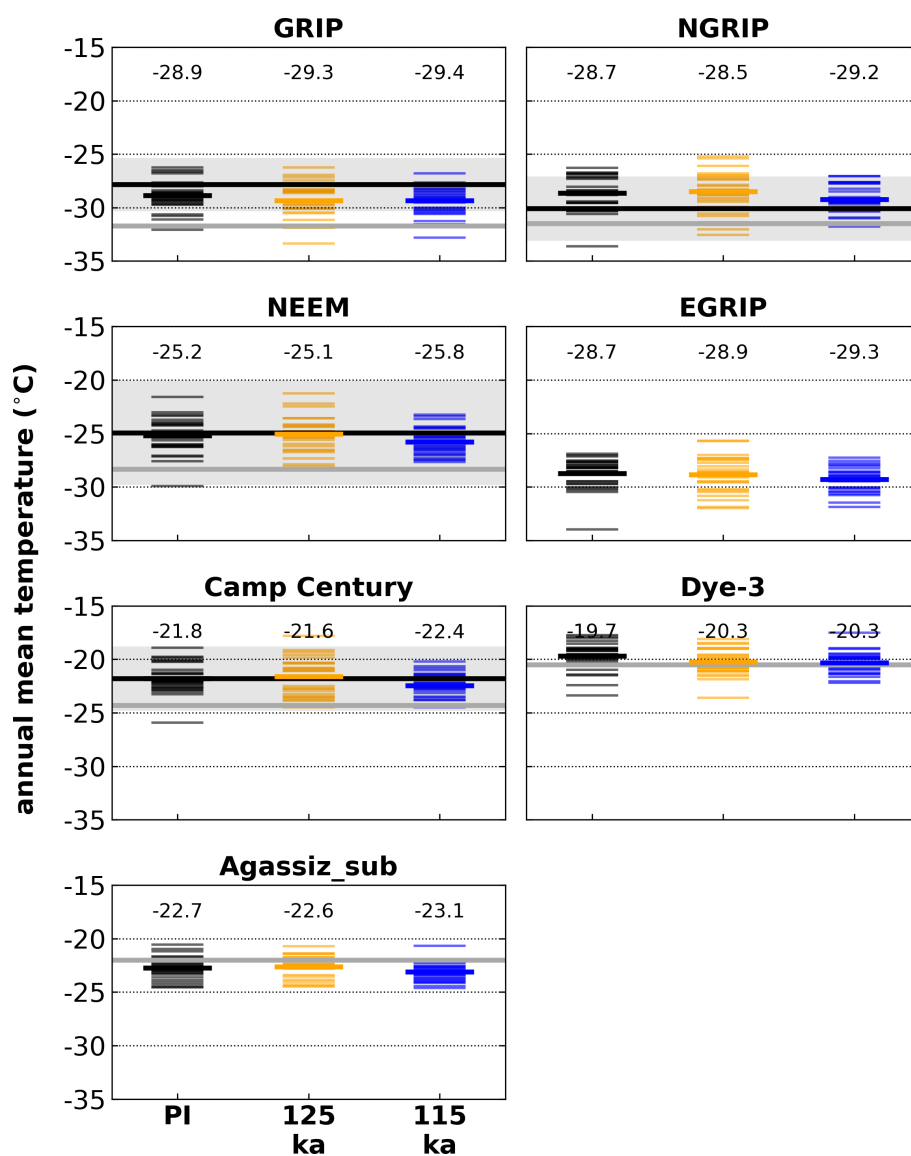


Figure 2. Annual mean (near-surface) temperature at Greenland ice core locations simulated by the climate model MAR for three time slices. Individual model years (short thin lines) and their mean (short bold lines, numerical values on top of columns) are compared to mean observations from weather stations (long bold lines in black), their corresponding standard deviation (gray shading), and 10 m borehole temperatures (annual mean; long bold lines in gray).

The simulated pre-industrial JJA (June-July-August) temperatures (Fig. 3; black columns; short bold lines - ensemble means; short thin lines - individual model years) also show good agreement with observations from weather stations (Fig. 3, long bold lines in black). The climate simulations show consistently ~3-4 °C warmer temperatures (compared to pre-industrial; black) at all locations for mid Eemian conditions (125 ka: orange) and cooler temperatures for late Eemian conditions (115 ka: blue).

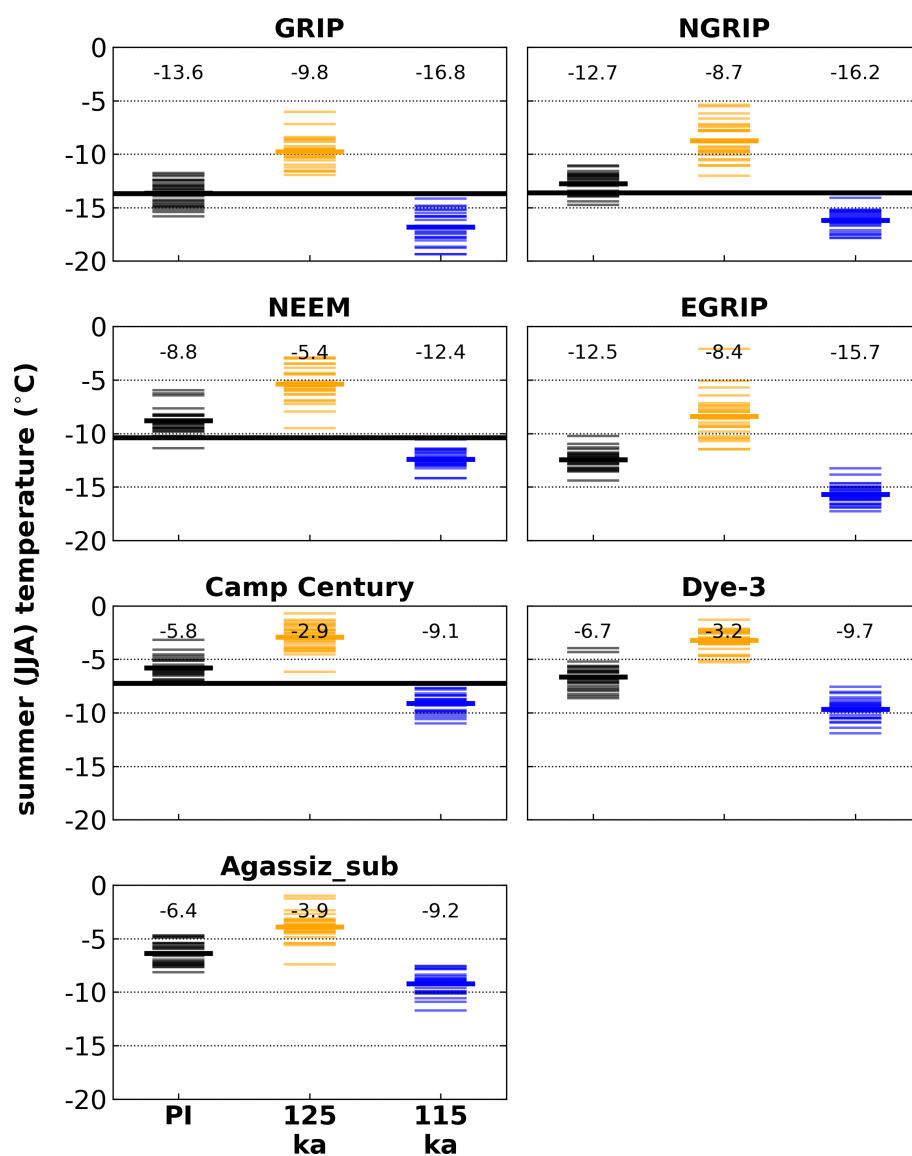


Figure 3. Mean (near-surface) JJA (June-July-August) temperature at Greenland ice core locations simulated by the climate model MAR for three time slices. Individual model years (short thin lines) and the mean (short bold lines, numerical value on top of columns) are compared to mean observations from weather stations (long bold lines in black).

The precipitation-weighted temperatures (Fig. A1), which is arguably closer to what is recorded in an ice core, show a similar pattern as the JJA temperatures (Fig. 3). However, the precipitation-weighted temperatures show a less pronounced warming for mid Eemian conditions (125 ka: orange), i.e., maximum 3 °C warmer compared to pre-industrial (black).



Number of melt days

Passive microwave satellite data shows a strong difference in observed melt days per year (i.e., presence of surface water) (Fig. 4; first three columns from the left; brown and green) between central ice core locations (NEEM, EGRIP, NGRIP, GRIP), where surface melt is sparse, and locations closer to the margins (Camp Century, Dye-3) and ice caps (Agassiz), where melt is much more frequent. Central locations show between 0 and ~ 1 melt days year⁻¹ in the last ~ 30 years for which satellite data are available. The exact values vary depending on the location, satellite data set, and whether the extreme melt event of 2012 is included.

The simulated pre-industrial melt day frequency (Fig. 4, black columns) shows good agreement with the observations (Fig. 4; brown and green columns), i.e., low melt frequencies at the central locations and higher melt frequencies at locations at the margins. However, the simulated pre-industrial melt frequencies are in general lower than present-day observations (especially at the Agassiz location), with the exception of Dye-3 which shows a higher simulated melt frequency.

Melt and refreezing

The 125 ka simulations (Fig. 4; orange columns) show a significantly higher melt frequency at all locations (more than 30 melt days year⁻¹ at Dye-3), compared to the pre-industrial simulations (Fig. 4; black columns) and observations (Fig. 4; brown/green columns). The SMB simulations show surface melt at all ice core locations during the warm mid Eemian with an annual melt water production (Fig. A2) for warmer locations of ~ 300 – 400 mm w.e. year⁻¹ (Camp Century) and ~ 600 – 700 mm w.e. year⁻¹ (Dye-3). However, even modern dry, high altitude locations show an annual surface melt of ~ 100 mm w.e. year⁻¹ (GRIP, NGRIP, EGRIP). NEEM shows ~ 200 mm w.e. year⁻¹ for the warmest Eemian simulations.

The simulated mean amount of refreezing exceeds 40 % of the annual accumulation at most ice core locations under warm mid Eemian conditions (Fig. 5; red and orange columns). Even the highest location, GRIP at ~ 3200 m elevation, shows more than 25% refreezing under 125 ka conditions. The largest amount of refreezing is simulated at Dye-3, EGRIP, and Agassiz_sub where refreezing percentage reaches 90% and more.

Total air content (TAC)

Theoretical TAC derived from simulated surface pressure and annual mean temperature (Raynaud et al., 1997) and reduced according to the amount of simulated refreezing (Fig. 6 and Sec. 2) shows significantly lower values for the 125 ka simulations. Most of the higher ice core locations (GRIP, NGRIP, NEEM, and Camp Century) show simulated TAC values between 50 and 60 ml kg⁻¹, whereas the respective pre-industrial values are between 90 and 100 ml kg⁻¹. At Dye-3 the simulated TAC is lower than 20 ml kg⁻¹ for the warm 125 ka Eemian simulations. Observed Holocene TAC from ice core records (Fig. 6; horizontal gray shading) fit well with the pre-industrial simulations, while observed Eemian TAC (Fig. 6; horizontal orange shading) is not as low as the simulated values.

Finally, TAC observations from the deeper ice core sections (i.e., possibly Eemian; Fig. 7; NEEM, GRIP, NGRIP; circles) are compared with mean simulated TAC for 115 ka (Fig. 7; blue line) and 125 ka conditions (Fig. 7; orange line). For Dye-3

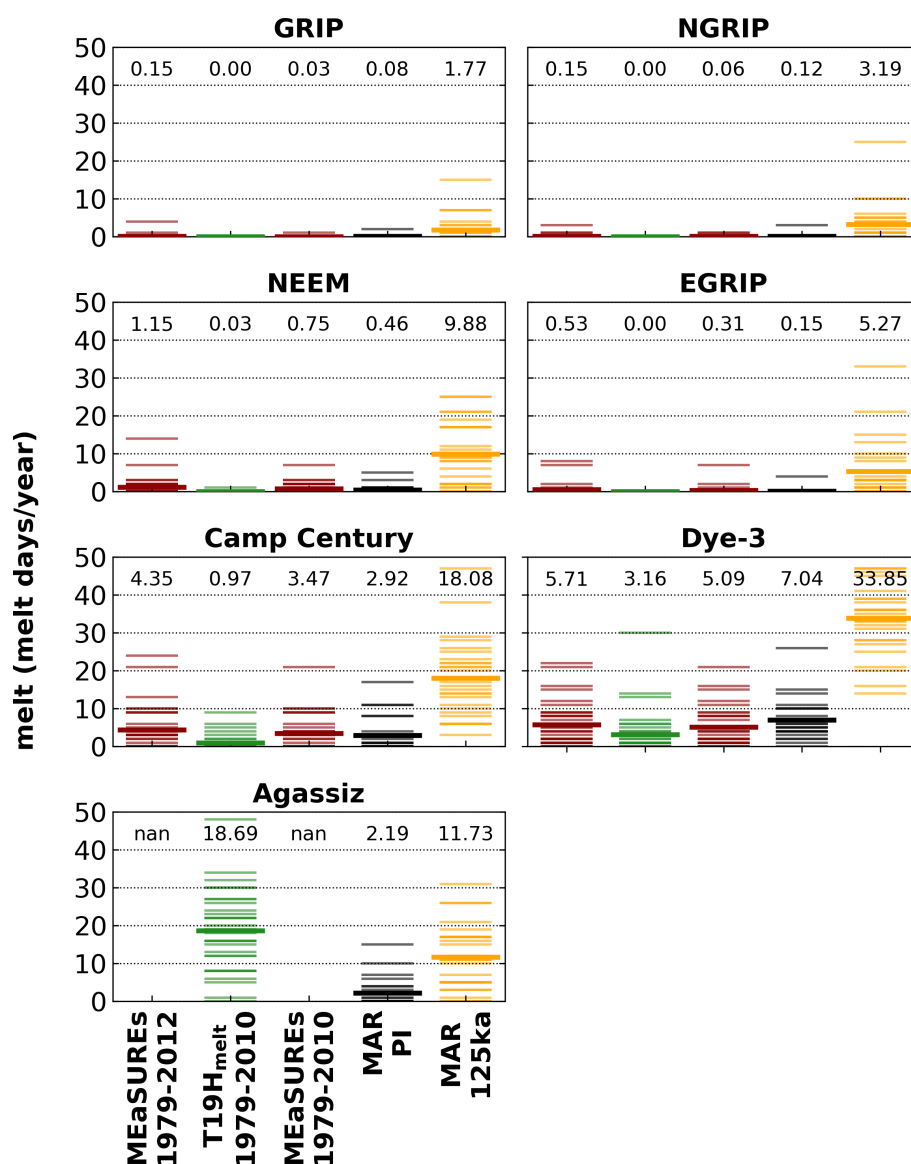


Figure 4. Annual melt days at Greenland ice core locations derived from satellite data and simulated by the climate model MAR. Observations in the first three columns from the left are compared with simulations in the fourth and fifth column. Columns from the left: (1) Passive microwave data from MEaSUREs (1979 to 2012); (2) The same data as in (1) but with a different processing (T19H_{melt}; Fettweis et al., 2011) (1979 to 2010); (3) the MEaSUREs data set excluding the extreme melt year 2012 (1979 to 2010); (4) Simulated melt for pre-industrial (PI) and (5) 125 ka conditions. Individual model years (thin lines) and the ensemble means (bold lines, numerical values on top of columns) are shown. For Agassiz, simulation results for the substitute location are shown; as discussed in Sec. 2.

the entire TAC record is shown due to the lack of Eemian observations. Note: NEEM and GRIP are shown against age based

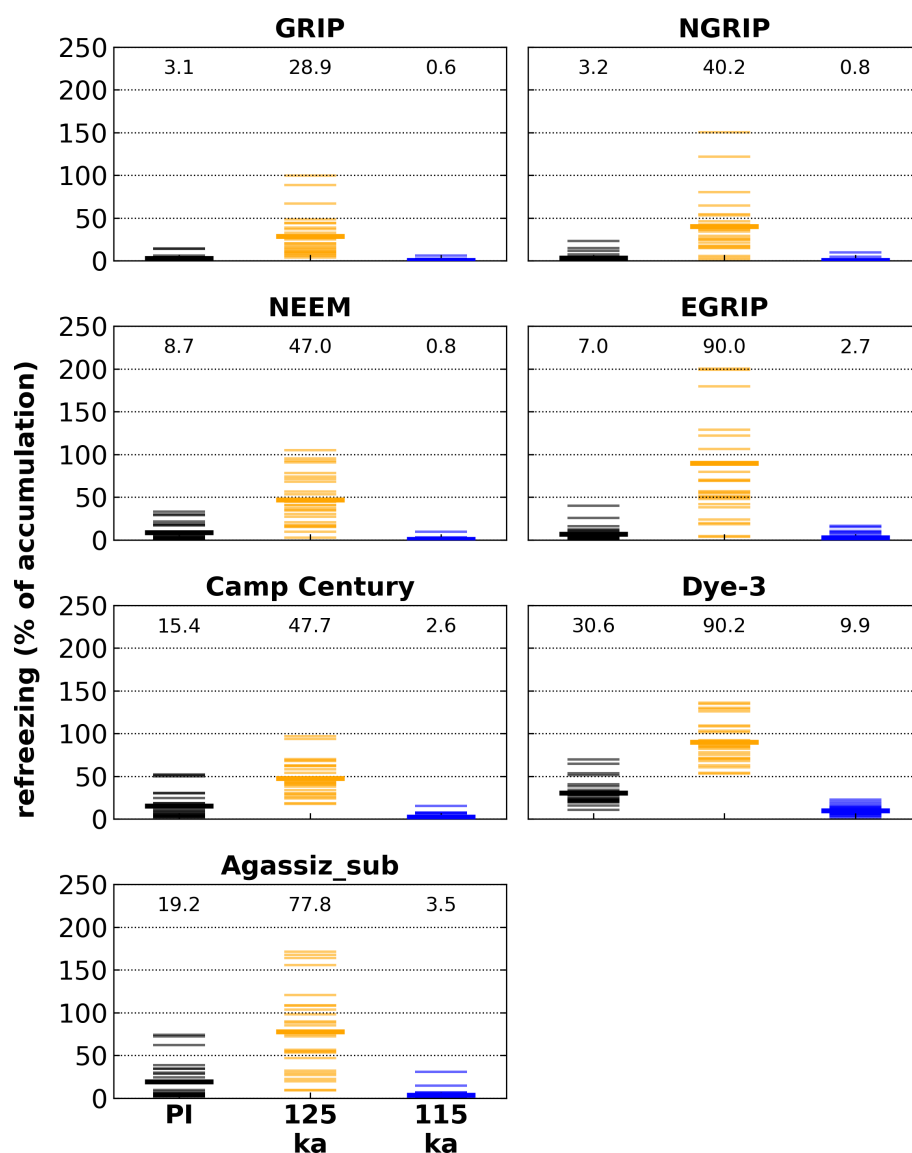


Figure 5. Annual refreezing percentage (of accumulation) at Greenland ice core locations simulated by the climate model MAR for three time slices. Individual model year percentages (thin lines) and the simulation ensemble mean percentages (bold lines, numerical values on top of columns) are shown.

on a more robust chronology involving "unfolding the ice" (NEEM community members, 2013; Landais et al., 2003), while
 175 NGRIP and Dye-3 are shown against core depth.

The 115 ka simulations generally fit well with the late Eemian (NEEM, GRIP, NGRIP) and Holocene (Dye-3) observations. While the 125 ka simulations are lower than the observations. For the NEEM data, the lowest TAC observation are within the gray shading which indicates the influence of melt at the ice core site (NEEM community members, 2013).

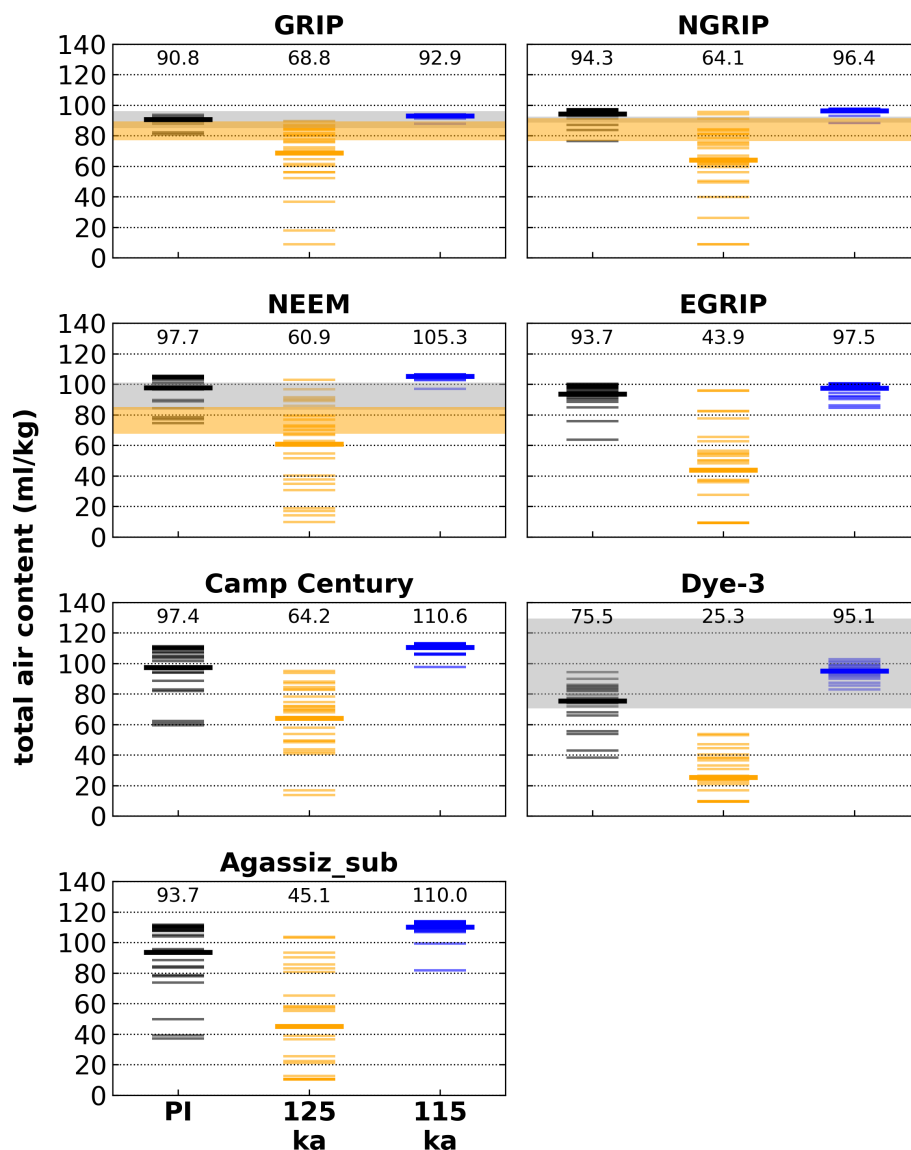


Figure 6. Calculated TAC at Greenland ice core locations derived from simulations with the climate model MAR for three time slices (see method in Sec. 2). Individual model years (thin lines) and the simulation ensemble means (bold lines, numerical values on top of columns) are compared to observed late Holocene and Eemian ranges (horizontal gray and orange shading, respectively; two standard deviations). Note: The Holocene range at NGRIP is very narrow and almost completely overlapping with the respective Eemian range and there is no Eemian range for Dye-3.

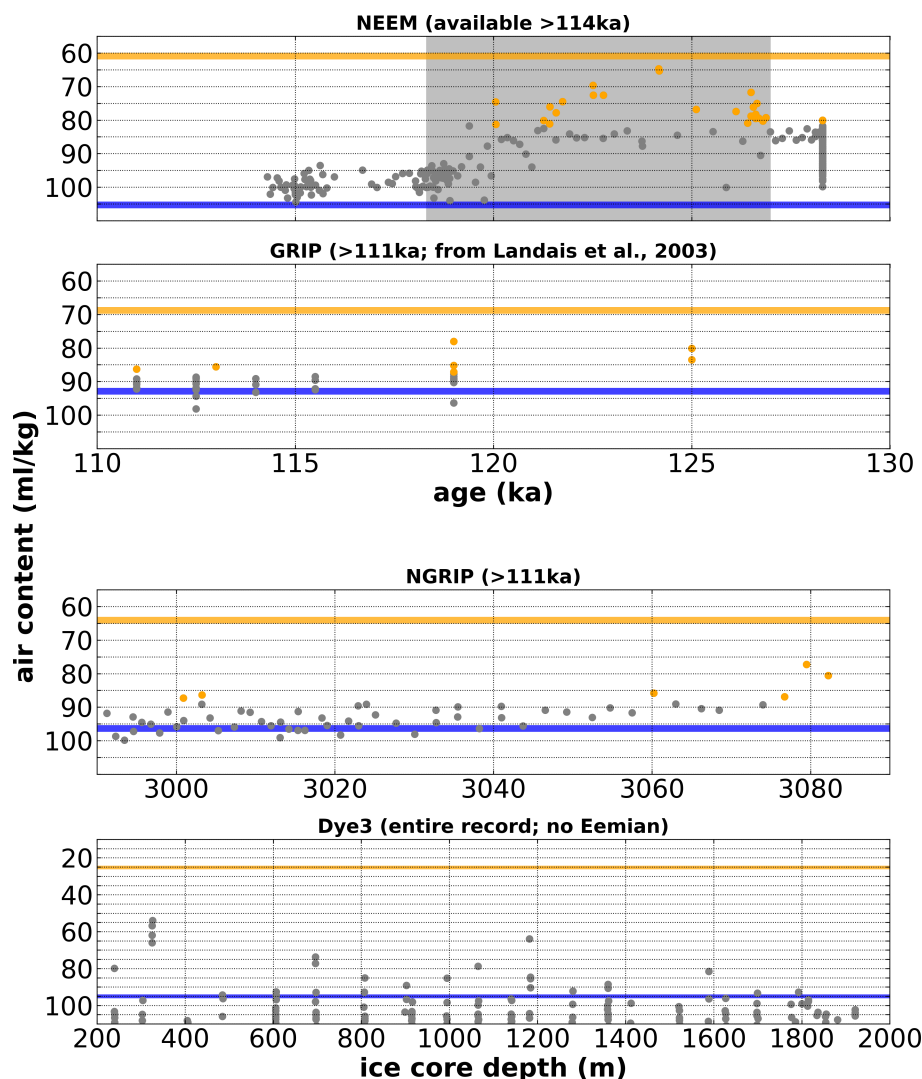


Figure 7. Observed TAC from four Greenland ice cores — NEEM, GRIP, NGRIP, Dye-3. Observations (circles) are compared with mean simulated TAC for 115 ka (blue horizontal lines) and 125 ka simulations (orange horizontal lines). Data points used to calculate the Eemian range in Fig. 6 are indicated with orange circles. Note: NEEM and GRIP are shown against age due to their robust age model, while NGRIP and Dye-3 are shown against ice core depth. The NEEM melt zone (NEEM community members, 2013) is highlighted with a gray shading. The y-axes are reversed.

4 Discussion

180 The enhanced Eemian seasonality (Yin and Berger, 2010) and warmer Eemian summers (CAPE Last Interglacial Project Members, 2006; Otto-Bliesner et al., 2013; Capron et al., 2014) are indicators of elevated melt during this period. The recent extreme melt event in Greenland in 2012 and a similar event in 1889 (Nghiem et al., 2012) demonstrate that surface melt on



the entire Greenland ice sheet, even at the summit of Greenland, is possible under recent climate conditions. Even though these extreme Greenland-wide melt events were caused by a rare large-scale atmospheric pattern (Neff et al., 2014) and were further enhanced by an externally caused albedo lowering (ash deposition from forest fires; Keegan et al., 2014), it is likely that such events are more frequent in a warmer climate such as the Eemian interglacial period.

The simulations discussed in this study (regional climate plus a full surface energy balance) indicate surface melt and refreezing (Fig. 4 and 5) at all deep Greenland ice core locations. Even central Greenland locations close to Summit show a melt of 100 mm year⁻¹ (Fig. A2). Due to this surface melt, TAC derived from these simulations are between ~25 % (GRIP) and ~80 % (Dye-3, EGRIP) lower than modern (pre-industrial) values (Fig. 6). Even though the presented climate simulations show such extensive melt, there are several reasons why these simulations can be interpreted as conservative estimates: (1) The simulated pre-industrial melt frequency is mostly lower than satellite observations (Fig. 4; black versus brown/green columns). However, the observation of higher melt frequencies can likely also be related to the effects of recent global warming which are not represented in the pre-industrial climate simulations. (2) Processes like ash deposition which were partly responsible for the extreme Greenland melt events of 2012 and 1889 (Keegan et al., 2014) are not simulated. (3) The climate simulations do not include a lowering of the Eemian ice sheet surface which would likely enhance the simulated warming.

Furthermore, the absence of a simulated annual warming, and proxy data showing Eemian peak temperatures as high as +7.5 ± 1.8 °C (NEEM community members, 2013, without altitude corrections) and +8.5 ± 2.5 °C (Landais et al., 2016) for NEEM (the North Greenland Eemian Ice Drilling project in northwest Greenland), and +5.2 ± 2.3 °C (Landais et al., 2016, lower bound as the record only starts after the peak Eemian warming) for NGRIP (North Greenland Ice Core Project) indicate that the climate simulations might be cold. The simulated JJA temperatures (Fig. 3) and the simulated precipitation-weighted temperatures (Fig. A1) show a peak warming of only ~3–4 °C and ~3 °C, respectively. However, the fact that NEEM community members (2013) infer an elevation (at the deposition site) of several hundred metres higher than at NEEM today complicates the interpretation of how well the simulated temperatures fit the proxy-derived observations. If the estimated NEEM deposition site was lower than inferred, e.g., stronger influenced by melt, then the warming of ~8 °C at constant elevation would be too high and the simulations would fit better.

Focusing again on the comparison of melt observations and simulations (Fig. 4), a strong underestimation of melt at the Agassiz site in the pre-industrial simulations becomes apparent. This strong underestimation is likely related to the fact that a substitute location for the ice cap is used, i.e., a model location with similar model and observed elevation is chosen. The selection of the substitute location is necessary, because the low model topography at the original core locations causes unrealistically high melt simulations. Furthermore, the Agassiz site is only covered by the satellite data which appears to be less sensitive to melt (T19H_{melt}), i.e., T19H_{melt} shows less melt than MEaSUREs at all investigated locations. And although Eemian ice is absent at the Agassiz site, the simulated Eemian refreezing percentage (Fig. 5) of approximately 80% is consistent with the Agassiz melt record which indicates 100% melt during the Holocene optimum ~10–11 ka (Fisher et al., 2012; Lecavalier et al., 2017).

Another important aspect for the interpretation of the simulated melt is the formation of melt layers and the amount of meltwater needed to form a (visible) melt layer. While the presented TAC calculations assume Henry's solubility law (Sander,



2015) for the air content of the melt layer, the formation of a melt layer in an ice core is a complicated process, e.g., depending on prevailing snow properties. A higher number of melt layers is not just the result of uniformly higher summer temperatures, but the result of an increased contrast between the pre-melt snow pack temperatures (strongly influenced by winter temperature) and the summer melt rate (a function of summer temperature) (Pfeffer and Humphrey, 1998). Therefore, the enhanced Eemian seasonality might have been favourable for the formation of melt layers.

The simulated TACs for 125 ka conditions are mostly lower than the observations (Fig. 6 and 7) particularly at GRIP, NGRIP, and Dye-3. At NEEM on the other hand — the ice core with the most complete Eemian record (likely including peak warming) — the simulated 125 ka TAC matches well with the lowest observations, indicating that the high amount of simulated melt could explain these observations. The variability of the observed NEEM TAC in the suggested melt zone between 127 and 118.3 ka (gray shading; NEEM community members, 2013) is large, likely due to the varying influence (i.e., number) of melt layers.

The Eemian TAC measurements at GRIP and NGRIP also show reduced values (not as low as at NEEM), which can be interpreted in a similar way as at NEEM — GRIP and NGRIP might have been influenced by Eemian melt as well. The simulated 125 ka TAC for both locations are strongly reduced (relative to pre-industrial levels), but do not reach levels as low as at NEEM. However, these reduced TAC levels could still indicate significant surface melt.

Overall the lack of a better agreement between observed and simulated Eemian TAC (i.e., few TAC observations as low as the simulations) could be related to the sparse number of Eemian peak warming observations (most ice core records only start after the peak warming; particularly at GRIP, NGRIP, and Dye-3). However, another possible explanation could be a shift of the precipitation rates in central Greenland towards much higher values during the Eemian interglacial period. Unfortunately, accumulation rates are unconstrained for the Eemian sections of Greenland ice cores.

Furthermore, another uncertainty to the interpretation of the simulations is the effect of the higher Eemian summer insolation on the TAC. An anti-correlation between local summer insolation and TAC is known in ice core records from East Antarctica during the last 400000 years (Raynaud et al., 2007) and the insolation signal is also found in Greenlandic TAC (NGRIP, Eicher et al., 2016). NEEM community members (2013) estimate (based on data from the Holocene optimum) that the summer insolation could account for 50% of the observed Eemian TAC changes at NEEM.

Nevertheless, the possibility of a melt-induced reduction of TAC should be considered for the interpretation of Eemian air content as ice surface elevation changes. An early interpretation of the first Greenland ice cores (Camp Century, Dye-3) suggested an extreme scenario for Eemian Greenland with extensive melt of the entire ice sheet and a much smaller ice sheet leading to a sea level rise of 6 m (Koerner, 1989). However, this scenario was rejected by later ice core studies showing evidence of Eemian ice (especially NGRIP and NEEM; North Greenland Ice Core Project members et al., 2004; NEEM community members, 2013). Furthermore, GRIP TAC measurements (Raynaud, 1999) have been interpreted as evidence for the elevation of the summit sites having remained above 3000 m of altitude during the Eemian and GRIP deuterium excess measurements remain in the normal range during the Eemian (Landais et al., 2003). However, this last interpretation can be challenged by measurements of a NEEM Holocene melt layer, suggesting that the melt layer mainly influences TAC and CH₄ observations, while other variables like deuterium excess may be less influenced by melt (NEEM community members, 2013).



The climate simulations show surface melt at all deep ice core locations and at the Agassiz ice cap under 125 ka climate conditions (Fig. 4 and A2; orange column). Even locations near the summit of Greenland (NGRIP and GRIP) show several melt days (i.e., $>8 \text{ mm day}^{-1}$) during these warm Eemian simulations. NEEM, the ice core location with the longest Eemian record, shows ~ 10 melt days year^{-1} . While the presence of Eemian surface melt at NEEM was acknowledged previously (NEEM community members, 2013), the lower TAC observations at GRIP and NGRIP could as well be related to Eemian surface melt, rather than stable or higher elevations.

Furthermore, it should be emphasized that a robust estimate of Eemian Greenland surface melt is challenging to accomplish with the results of a single climate model. It would be highly advantageous to have an ensemble of climate to explore model biases and uncertainties. However, as pointed out earlier in this discussion, there are several reasons why the presented climate simulations could be interpreted as conservative in terms of Eemian melt. It is likely that there are other climate models which might show more extensive Eemian surface melt.

In the future, an analysis of individual or ensemble Eemian climate simulations would benefit from a comparison of the observed extreme melt event in 2012 with simulated extreme melt events. Relationships between simulated variables such as surface air temperature and local wind patterns, and the simulated melt could be analyzed and then be used in order to identify specific weather patterns leading to the simulated high surface melt on Greenland.

5 Conclusions

The regional climate simulations (including a full surface energy balance) discussed in this study show surface melt at all Greenland ice core locations during the Eemian interglacial period. The amount of simulated refreezing exceeds 25 % of the annual accumulation at the summit of Greenland (GRIP) and reaches values as high as 90 % at less central locations like Dye-3 and EGRIP. The simulated air pressure, temperature, and refreezing are used to calculate estimates of Eemian total air content which could explain the lowest corresponding ice core observations. This is true even though the discussed simulations could show conservative melt estimates, i.e., the simulations neglect processes which would likely increase the melt. Therefore, the possibility of widespread surface melt should be considered for the interpretation of Greenlandic total air content records from warm periods such as the Eemian interglacial period. In the future, a robust map of Eemian melt estimates in Greenland could be used in combination with patterns of accumulation to identify potential sites for future Greenland ice cores. This procedure would increase the chances of finding well preserved Eemian ice without or with less influence by melt layers. These sites will have relatively high accumulation combined with low surface melt.

6 Code availability

The MAR code is available at: <http://mar.cnrs.fr> (last access: 25.05.2020)



7 Data availability

The Eemian MAR simulations are available from the corresponding author upon request. *MEaSUREs Greenland Surface Melt Daily 25km EASE-Grid 2.0, Version 1* (Mote, 2014) is freely available at: <https://nsidc.org/data/nsidc-0533/versions/1> (last access: 25.05.2020). For more information and to request the T19H_{melt} data (Fettweis et al., 2011) please contact Xavier Fettweis (xavier.fettweis@uliege.be). For more information and to request the collection of Greenland shallow ice core and weather station data (Faber, 2016) please contact Anne-Katrine Faber (anne-katrine.faber@uib.no). The TAC observations at NEEM (NEEM community members, 2013) are freely available at: <http://www.iceandclimate.nbi.ku.dk/data/> (last access: 25.05.2020). The GRIP TAC (Raynaud, 1999) is freely available at: <https://doi.pangaea.de/10.1594/PANGAEA.55086> (last access: 25.05.2020). The NGRIP TAC (Eicher et al., 2016) is freely available at: <https://www.ncdc.noaa.gov/paleo-search/study/20569> (last access: 25.05.2020). For more information and to request the Dye-3 data, please contact Sindhu Vudayagiri (sindhu.v@nbi.ku.dk).

Appendix A: Appenix A

Author contributions. AP and BMV designed the study with contributions from KHN. Dye-3 total air content data was extracted from Fig. 4 in Herron and Langway (1987) by SV. AP made the figures and wrote the text with input from BMV, KHN, SV, and TB.

Competing interests. The authors declare that they have no conflict of interest.

Acknowledgements. The research leading to these results has received funding from the European Research Council under the European Community's Seventh Framework Programme (FP7/2007-2013) / ERC grant agreement 610055 as part of the ice2ice project. We thank Chuncheng Guo for performing the Eemian NorESM simulations and Sébastien Le clec'h for downscaling the NorESM simulations with the regional model MAR. Furthermore, we would like to thank Anne-Katrine Faber for valuable discussions and providing the shallow ice core data she compiled during her PhD. We also thank Xavier Fettweis for providing the T19H_{melt} data.

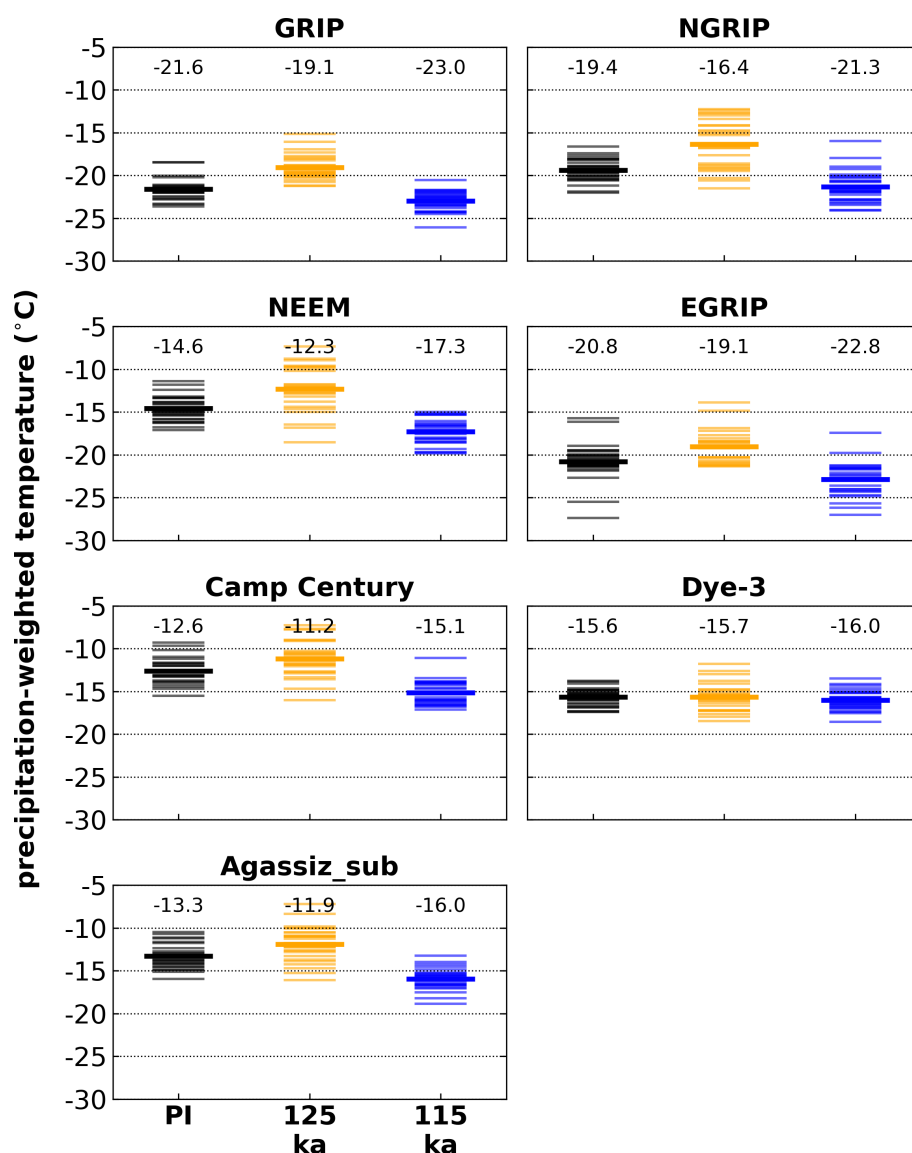


Figure A1. Annual mean precipitation-weighted temperature at Greenland ice core locations simulated by the climate model MAR for three time slices. Individual model years (thin lines) and the mean (bold lines, numerical values on top of columns) are shown.

References

- Alley, R. B. and Anandakrishnan, S.: Variations in melt-layer frequency in the GISP2 ice core: implications for Holocene summer temperatures in central Greenland, https://www.igsoc.org/annals/21/igs_annals_vol21_year1995_pg64-70.pdf, 1995.
- 305 Alley, R. B. and Koci, B. R.: Ice-Core Analysis at Site A, Greenland: Preliminary Results, *Annals of Glaciology*, 10, 1–4, <https://doi.org/10.3189/S0260305500004067>, 1988.

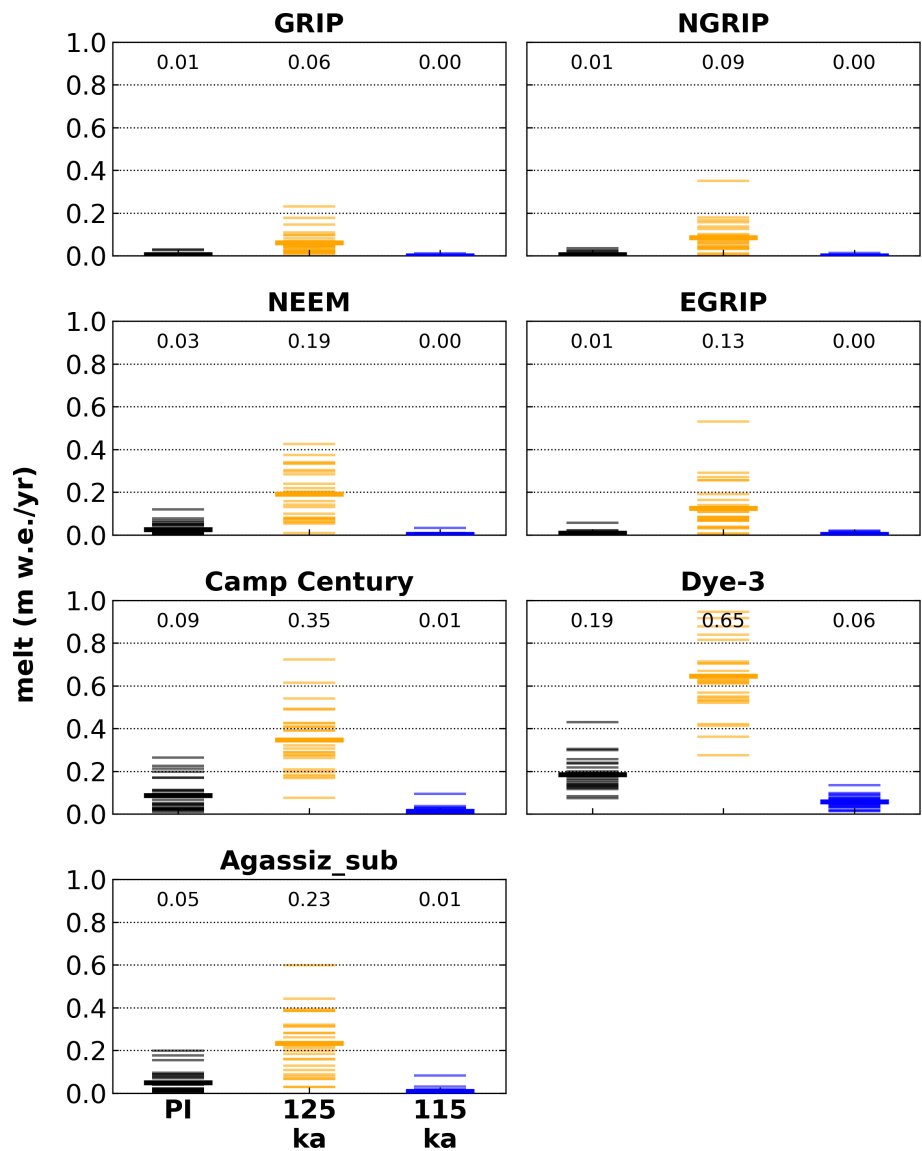


Figure A2. Annual melt at Greenland ice core locations simulated by the climate model MAR for three time slices. Individual model years (thin lines) and the mean (bold lines, numerical values on top of columns) are shown.

CAPE Last Interglacial Project Members: Last Interglacial Arctic warmth confirms polar amplification of climate change, *Quaternary Science Reviews*, 25, 1383–1400, <https://doi.org/10.1016/j.quascirev.2006.01.033>, 2006.

Capron, E., Govin, A., Stone, E. J., Masson-Delmotte, V., Mulitza, S., Otto-Bliesner, B., Rasmussen, T. L., Sime, L. C., Waelbroeck, C., and Wolff, E. W.: Temporal and spatial structure of multi-millennial temperature changes at high latitudes during the Last Interglacial, *Quaternary Science Reviews*, 103, 116–133, <https://doi.org/10.1016/j.quascirev.2014.08.018>, 2014.

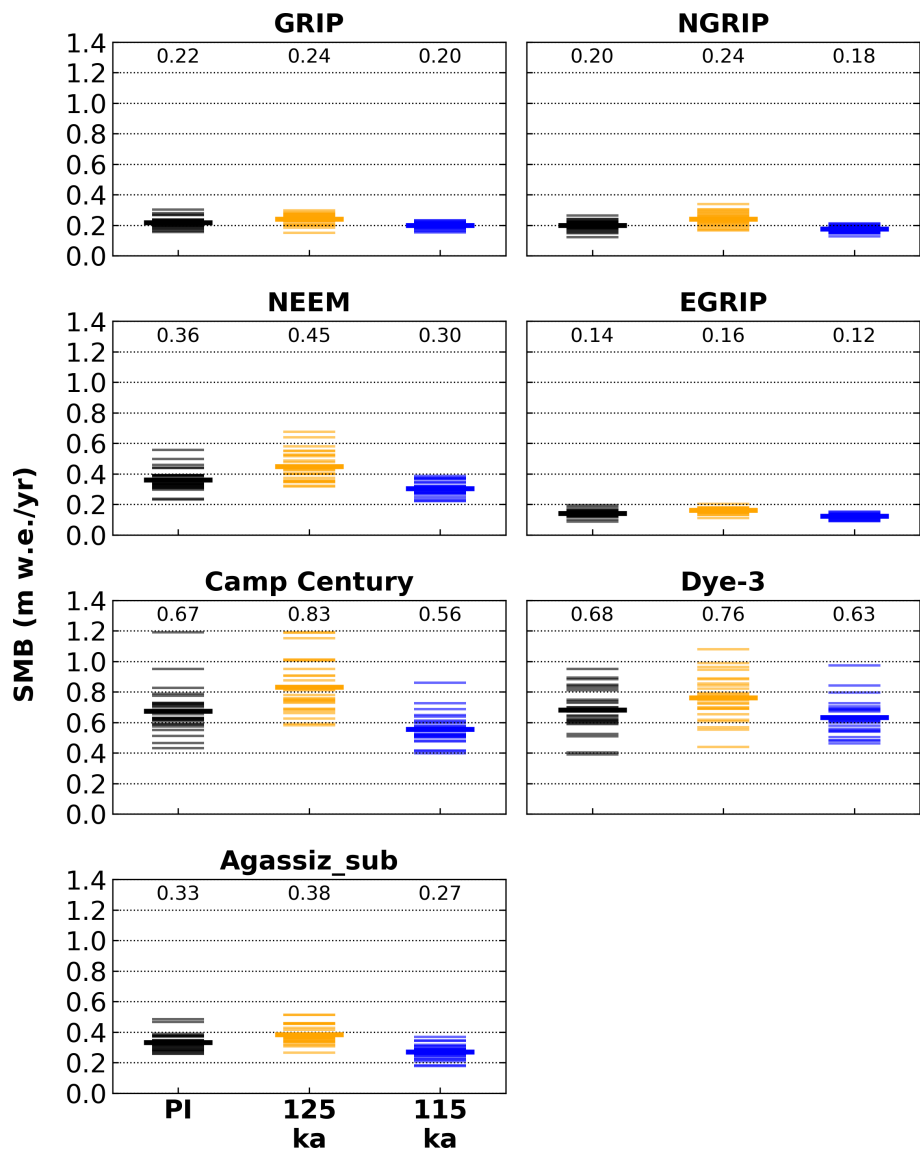


Figure A3. Annual Surface Mass Balance (SMB) at Greenland ice core locations simulated by the climate model MAR for three time slices. Individual model years (thin lines) and the mean (bold lines, numerical values on top of columns) are shown.

Eicher, O., Baumgartner, M., Schilt, A., Schmitt, J., Schwander, J., Stocker, T. F., and Fischer, H.: Climatic and insolation control on the high-resolution total air content in the NGRIP ice core, *Clim. Past*, 12, 1979–1993, <https://doi.org/10.5194/cp-12-1979-2016>, 2016.

Faber, A.: Isotopes in Greenland precipitation. Isotope-enabled AGCM modelling and a new Greenland database of observations and ice core measurements, Ph.D. thesis, Centre for Ice and Climate, University of Copenhagen, 2016.

Fettweis, X.: Reconstruction of the 1979–2006 Greenland ice sheet surface mass balance using the regional climate model MAR, *The Cryosphere*, 1, 21–40, <https://doi.org/10.5194/tc-1-21-2007>, 2007.



- Fettweis, X., Tedesco, M., van den Broeke, M., and Ettema, J.: Melting trends over the Greenland ice sheet (1958–2009) from spaceborne microwave data and regional climate models, *The Cryosphere*, 5, 359–375, <https://doi.org/10.5194/tc-5-359-2011>, 2011.
- 320 Fettweis, X., Franco, B., Tedesco, M., Angelen, J. H. v., Lenaerts, J. T. M., Broeke, M. R. v. d., and Gallée, H.: Estimating the Greenland ice sheet surface mass balance contribution to future sea level rise using the regional atmospheric climate model MAR, *The Cryosphere*, 7, 469–489, <https://doi.org/10.5194/tc-7-469-2013>, 2013.
- Fettweis, X., Box, J. E., Agosta, C., Amory, C., Kittel, C., Lang, C., van As, D., Machguth, H., and Gallée, H.: Reconstructions of the 1900–2015 Greenland ice sheet surface mass balance using the regional climate MAR model, *The Cryosphere*, 11, 1015–1033, <https://doi.org/10.5194/tc-11-1015-2017>, 2017.
- 325 Fisher, D., Zheng, J., Burgess, D., Zdanowicz, C., Kinnard, C., Sharp, M., and Bourgeois, J.: Recent melt rates of Canadian arctic ice caps are the highest in four millennia, *Global and Planetary Change*, 84–85, 3–7, <https://doi.org/10.1016/j.gloplacha.2011.06.005>, 2012.
- Guo, C., Bentsen, M., Bethke, I., Ilicak, M., Tjiputra, J., Toniazzo, T., Schwinger, J., and Otterå, O. H.: Description and evaluation of NorESM1-F: A fast version of the Norwegian Earth System Model (NorESM), *Geoscientific Model Development Discussions*, pp. 1–37, <https://doi.org/10.5194/gmd-2018-217>, 2018.
- 330 Herron, S. L. and Langway, C. C.: Derivation of paleoelevations from total air content of two deep Greenland ice cores, p. 14, 1987.
- Keegan, K. M., Albert, M. R., McConnell, J. R., and Baker, I.: Climate change and forest fires synergistically drive widespread melt events of the Greenland Ice Sheet, *Proceedings of the National Academy of Sciences*, 111, 7964–7967, <http://doi.org/10.1073/pnas.1405397111>, 2014.
- 335 Koerner, R. M.: Ice Core Evidence for Extensive Melting of the Greenland Ice Sheet in the Last Interglacial, *Science*, 244, 964–968, <http://doi.org/10.1126/science.244.4907.964>, 1989.
- Landais, A., Chappellaz, J., Delmotte, M., Jouzel, J., Blunier, T., Bourg, C., Caillon, N., Cherrier, S., Malaizé, B., Masson-Delmotte, V., Raynaud, D., Schwander, J., and Steffensen, J. P.: A tentative reconstruction of the last interglacial and glacial inception in Greenland based on new gas measurements in the Greenland Ice Core Project (GRIP) ice core, *Journal of Geophysical Research: Atmospheres*, 108, <https://doi.org/10.1029/2002JD003147>, 2003.
- 340 Landais, A., Masson-Delmotte, V., Capron, E., Langebroek, P. M., Bakker, P., Stone, E. J., Merz, N., Raible, C. C., Fischer, H., Orsi, A., Prié, F., Vinther, B., and Dahl-Jensen, D.: How warm was Greenland during the last interglacial period?, *Clim. Past*, 12, 1933–1948, <https://doi.org/10.5194/cp-12-1933-2016>, 2016.
- Lecavalier, B. S., Fisher, D. A., Milne, G. A., Vinther, B. M., Tarasov, L., Huybrechts, P., Lacelle, D., Main, B., Zheng, J., Bourgeois, J., and Dyke, A. S.: High Arctic Holocene temperature record from the Agassiz ice cap and Greenland ice sheet evolution, *Proceedings of the National Academy of Sciences*, 114, 5952–5957, <https://doi.org/10.1073/pnas.1616287114>, 2017.
- 345 Martinerie, P., Raynaud, D., Etheridge, D. M., Barnola, J.-M., and Mazaudier, D.: Physical and climatic parameters which influence the air content in polar ice, *Earth and Planetary Science Letters*, 112, 1–13, [http://doi.org/10.1016/0012-821X\(92\)90002-D](http://doi.org/10.1016/0012-821X(92)90002-D), 1992.
- Martinerie, P., Lipenkov, V., Raynaud, D., Chappellaz, J., Barkov, N. I., and Lorius, C.: Air content paleo record in the Vostok ice core (Antarctica): A mixed record of climatic and glaciological parameters, *Journal of Geophysical Research: Atmospheres*, 99, 10 565–10 576, <https://doi.org/10.1029/93JD03223>, 1994.
- 350 Mote, T. L.: MEaSUREs Greenland Surface Melt Daily 25km EASE-Grid 2.0, Version 1. [Greenland subset], <https://doi.org/10.5067/MEASURES/CRYOSPHERE/nsidc-0533.001>, [25.08.2018], 2014.
- NEEM community members: Eemian interglacial reconstructed from a Greenland folded ice core, *Nature*, 493, 489–494, <https://doi.org/10.1038/nature11789>, 2013.
- 355



- Neff, W., Compo, G. P., Ralph, F. M., and Shupe, M. D.: Continental heat anomalies and the extreme melting of the Greenland ice surface in 2012 and 1889, *Journal of Geophysical Research: Atmospheres*, 119, 6520–6536, <https://doi.org/10.1002/2014JD021470>, 2014.
- Nghiem, S. V., Hall, D. K., Mote, T. L., Tedesco, M., Albert, M. R., Keegan, K., Shuman, C. A., DiGirolamo, N. E., and Neumann, G.: The extreme melt across the Greenland ice sheet in 2012: EXTREME MELT ACROSS GREENLAND ICE SHEET, *Geophysical Research Letters*, 39, <http://doi.org/10.1029/2012GL053611>, 2012.
- North Greenland Ice Core Project members, Andersen, K. K., Azuma, N., Barnola, J.-M., Bigler, M., Biscaye, P., Caillon, N., Chappellaz, J., Clausen, H. B., Dahl-Jensen, D., Fischer, H., Flückiger, J., Fritzsche, D., Fujii, Y., Goto-Azuma, K., Grønvold, K., Gundestrup, N. S., Hansson, M., Huber, C., Hvidberg, C. S., Johnsen, S. J., Jonsell, U., Jouzel, J., Kipfstuhl, S., Landais, A., Leuenberger, M., Lorrain, R., Masson-Delmotte, V., Miller, H., Motoyama, H., Narita, H., Popp, T., Rasmussen, S. O., Raynaud, D., Rothlisberger, R., Ruth, U., Samyn, D., Schwander, J., Shoji, H., Siggard-Andersen, M.-L., Steffensen, J. P., Stocker, T., Sveinbjörnsdóttir, A. E., Svensson, A., Takata, M., Tison, J.-L., Thorsteinsson, T., Watanabe, O., Wilhelms, F., and White, J. W. C.: High-resolution record of Northern Hemisphere climate extending into the last interglacial period, *Nature*, 431, 147–151, <http://doi.org/10.1038/nature02805>, 2004.
- Otto-Bliesner, B. L., Rosenbloom, N., Stone, E. J., McKay, N. P., Lunt, D. J., Brady, E. C., and Overpeck, J. T.: How warm was the last interglacial? New model–data comparisons, *Phil. Trans. R. Soc. A*, 371, 20130097, <https://doi.org/10.1098/rsta.2013.0097>, 2013.
- Pfeffer, W. T. and Humphrey, N. F.: Formation of ice layers by infiltration and refreezing of meltwater, *Annals of Glaciology*, 26, 83–91, <https://doi.org/10.3189/1998AoG26-1-83-91>, 1998.
- Plach, A., Nisancioglu, K. H., Le clec’h, S., Born, A., Langebroek, P. M., Guo, C., Imhof, M., and Stocker, T. F.: Eemian Greenland SMB strongly sensitive to model choice, *Clim. Past*, 14, 1463–1485, <https://doi.org/10.5194/cp-14-1463-2018>, 2018a.
- Plach, A., Nisancioglu, K. H., Langebroek, P. M., Born, A., and Le clec’h, S.: Eemian Greenland ice sheet simulated with a higher-order model shows strong sensitivity to surface mass balance forcing, *The Cryosphere*, 13, 2133–2148, <https://doi.org/10.5194/tc-13-2133-2019>, 2019.
- Raynaud, D.: GRIP total air content, PANGAEA, <https://doi.org/10.1594/PANGAEA.55086>, [last accessed: 25.09.2018], 1999.
- Raynaud, D., Chappellaz, J., Ritz, C., and Martinerie, P.: Air content along the Greenland Ice Core Project core: A record of surface climatic parameters and elevation in central Greenland, *Journal of Geophysical Research: Oceans*, 102, 26 607–26 613, <https://doi.org/10.1029/97JC01908>, 1997.
- Raynaud, D., Lipenkov, V., Lemieux-Dudon, B., Duval, P., Loutre, M.-F., and Lhomme, N.: The local insolation signature of air content in Antarctic ice. A new step toward an absolute dating of ice records, *Earth and Planetary Science Letters*, 261, 337–349, <https://doi.org/10.1016/j.epsl.2007.06.025>, 2007.
- Sander, R.: Compilation of Henry’s law constants (version 4.0) for water as solvent, *Atmospheric Chemistry and Physics*, 15, 4399–4981, <https://doi.org/10.5194/acp-15-4399-2015>, 2015.
- Souchez, R., Bouzette, A., Clausen, H. B., Johnsen, S. J., and Jouzel, J.: A stacked mixing sequence at the base of the Dye 3 Core, Greenland, *Geophysical Research Letters*, 25, 1943–1946, <https://doi.org/10.1029/98GL01411>, 1998.
- Vinther, B. M., Clausen, H. B., Fisher, D. A., Koerner, R. M., Johnsen, S. J., Andersen, K. K., Dahl-Jensen, D., Rasmussen, S. O., Steffensen, J. P., and Svensson, A. M.: Synchronizing ice cores from the Renland and Agassiz ice caps to the Greenland Ice Core Chronology, *Journal of Geophysical Research: Atmospheres*, <https://doi.org/10.1029/2007JD009143>, 2008.
- Vinther, B. M., Buchardt, S. L., Clausen, H. B., Dahl-Jensen, D., Johnsen, S. J., Fisher, D. A., Koerner, R. M., Raynaud, D., Lipenkov, V., Andersen, K. K., Blunier, T., Rasmussen, S. O., Steffensen, J. P., and Svensson, A. M.: Holocene thinning of the Greenland ice sheet, *Nature*, 461, 385–388, <https://doi.org/10.1038/nature08355>, 2009.



Yin, Q. Z. and Berger, A.: Insolation and CO₂ contribution to the interglacial climate before and after the Mid-Brunhes Event, Nature
395 Geoscience, 3, 243–246, <https://doi.org/10.1038/ngeo771>, 2010.